BILINGUAL PUBLISHING GROUP

Journal of Building Material Science

https://journals.bilpubgroup.com/index.php/jbms

ARTICLE

Effect of Date Palm Fiber Content on the Tensile Behavior of Epoxy/Date Palm Fiber Bio-Composites: Experimental Investigation and Finite Element Analysis

Ikram Issami [1], *Ltaief Lammari* [2*], *Ali Rakrouk* [2], *Sana Ben Khlifa* [2], *Khaled El Moueddeb* [2], *Rachid Nasri* [2]

[1] *LR11ES19 Applied Mechanics and Engineering Laboratory, National School of Engineers of Tunis, University of Tunis El Manar, Tunis 1002, Tunisia*

[2] *Mechanical and Agro-Industrial Engineering Laboratory, Higher School of Engineering of Medjez El Bab, University of Jendouba, Medjez El Bab 9070, Tunisia*

ABSTRACT

Natural fiber-reinforced composites have attracted considerable attention as environmentally sustainable substitutes for conventional synthetic materials. Nevertheless, determining an appropriate fiber loading remains a critical issue, since higher reinforcement contents may improve stiffness while adversely affecting ductility and overall mechanical behavior. In the present work, the tensile performance of epoxy composites reinforced with untreated date palm fibers (DPFs) collected from southern Tunisia was investigated through a combination of experimental tensile tests and finite element analysis (FEA). Four fiber mass fractions (5, 10, 15, and 20 wt.%) were considered to evaluate the influence of reinforcement content on the mechanical response of the developed bio-composites. The experimental findings revealed a progressive increase in tensile strength, from 25.3 MPa at 5 wt.% fiber content to 31.6 MPa at 20 wt.%, while the Young's modulus increased from 2.0 GPa to 3.67 GPa. Conversely, the strain at failure decreased from 4.8% to 2.5%, reflecting a gradual loss of deformability as the fiber fraction increased. The formulations containing 10 wt. % and 15 wt.% fibers provided a favorable compromise between stiffness, strength, and deformation capability. The numerical predictions obtained from

*CORRESPONDING AUTHOR:
Ltaief Lammeri, Mechanical and Agro-Industrial Engineering Laboratory, Higher School of Engineering of Medjez El Bab, University of Jendouba, Medjez El Bab 9070, Tunisia; Email: ltaieflammmari@gmail.com

ARTICLE INFO
Received: 20 April 2026 | Revised: 12 May 2026 | Accepted: 11 June 2026 | Published Online: 22 June 2026
DOI: https://doi.org/10.30564/jbms.v8i2.13432

CITATION
Issami, I., Lammeri, L., Rakrouk, A., et al., 2026. Effect of Date Palm Fiber Content on the Tensile Behavior of Epoxy/Date Palm Fiber Bio-Composites: Experimental Investigation and Finite Element Analysis. Journal of Building Material Science. 8(2): 93–111. DOI: https://doi.org/10.30564/jbms.v8i2.13432

the homogenized linear elastic FEA model showed good agreement with the experimental results, with coefficients of determination (R^2) of 0.979 for tensile stress prediction and 0.994 for strain prediction. The proposed numerical approach provided a reasonable macroscopic approximation of the tensile response despite the simplified homogenization assumptions adopted. The novelty of this work lies in the combined experimental–numerical investigation of untreated Tunisian date palm fiber/epoxy bio-composites and the assessment of the applicability and limitations of a simplified homogenized FEA approach for predicting their tensile behavior.

Keywords: Bio-Composite; Date Palm Fibers; Epoxy Composite; Finite Element Analysis (FEA); Tensile Behavior; Sustainable Materials

1. Introduction

Over the past few decades, composite materials have attracted considerable industrial interest because of their ability to combine lightweight characteristics with high mechanical performance. In particular, polymer matrix composites reinforced with synthetic fibers such as glass and carbon fibers have progressively emerged as alternatives to conventional metallic materials in several engineering sectors, including automotive, aerospace, packaging, marine, and electronics industries [1,2]. Their widespread use is mainly associated with their high stiffness, corrosion resistance, and relatively good durability under severe service conditions.

A significant limitation of synthetic fiber reinforcements lies in their relatively high density. Glass fibers typically possess a density close to 2.5 g/cm^3, whereas carbon fibers generally range from 1.7 to 2.0 g/cm^3 [3]. The resulting increase in structural weight has a direct impact on fuel consumption and associated carbon emissions, particularly in sectors such as transportation, where weight reduction remains a key design objective. Furthermore, synthetic composites are predominantly produced from petroleum-based resources and often present considerable challenges at the end of their service life due to limited recyclability. Their production also requires substantial energy input and is associated with environmental burdens related to greenhouse gas emissions and waste generation [4,5].

In response to these limitations, growing research efforts have focused on natural fiber-reinforced polymer composites (NFRPCs) as alternative engineering materials. These composites combine plant-derived reinforcements with polymer matrices to obtain lightweight structures with a reduced environmental footprint. Natural fibers are particularly attractive because of their low density, renewable origin, biodegradability, broad availability, and relatively low processing cost [6–8]. Depending on the botanical source, the density of lignocellulosic fibers generally ranges between 0.8 and 1.5 g/cm^3, remaining substantially lower than that of conventional glass fibers. Since many of these fibers are obtained from agricultural by-products and crop residues, their utilization also promotes resource recovery and supports circular economy practices.

Natural fibers can generally be classified into bast fibers (flax, hemp, jute, kenaf), leaf fibers (sisal, abaca, pineapple), seed fibers (cotton), fruit fibers (coir/coconut), stalk fibers, and agricultural residue fibers. Among the various agricultural residue fibers currently explored for composite applications, date palm fibers (DPFs) represent a particularly attractive reinforcement owing to their widespread availability and low economic value. Significant amounts of date palm biomass are generated each year in countries such as Tunisia, Algeria, Egypt, and Saudi Arabia, providing a readily accessible source of lignocellulosic reinforcement. The chemical composition of DPFs is dominated by cellulose, hemicellulose, and lignin, constituents that are largely responsible for their favorable specific mechanical properties and relatively low density [9].

The potential of incorporating natural fibers into polymer matrices has been widely explored as a means of enhancing material sustainability while maintaining acceptable mechanical performance. Previous investigations have shown that composites reinforced with DPFs can exhibit satisfactory tensile properties, reduced density, and interesting thermal insulation characteristics, making them suitable for both structural and semi-structural applications [10–12]. As a result, these materials have been considered for a variety of uses, including automotive interior components, lightweight construction panels, furniture elements, thermal insulation systems, packaging products, and sports equipment. Recent studies have also reported that the addition of DPFs to epoxy matrices contributes to increased stiffness while preserving adequate strength levels and reducing overall component weight [13]. Nevertheless, the mechanical response of such composites remains highly dependent on several factors, including fiber content, dispersion quality, interfacial bonding, surface condition, and processing parameters.

Alongside experimental characterization, numerical approaches have become valuable tools for analyzing the behavior of composite materials. Finite element analysis (FEA) provides insight into stress distribution, deformation patterns, and strain concentration zones under various loading conditions, while limiting the need for extensive experimental campaigns [14]. Numerous studies have successfully employed FEA to investigate natural fiber composites and predict their tensile response as well as the effectiveness of stress transfer mechanisms within the material [15–17]. However, most published numerical studies have focused on flax, hemp, jute, or sisal fiber composites. By contrast, finite element investigations dedicated to untreated date palm fiber-reinforced epoxy composites remain scarce, and experimental validation of the corresponding numerical predictions is still insufficiently documented.

The reinforcement used in this work consists of untreated date palm fibers obtained from pruning residues collected in southern Tunisia. These fibers were selected because they combine low density, local availability, and minimal acquisition cost. In many oasis regions of southern Tunisia, substantial quantities of date palm residues are generated annually and are frequently discarded or burned, creating environmental and management challenges. Their conversion into reinforcing elements for polymer composites therefore represents an attractive route for waste valorization, improved utilization of local resources, and the development of sustainable lightweight materials.

Within this framework, the present work examines the tensile behavior of epoxy bio-composites reinforced with untreated date palm fibers through a combined experimental and numerical approach. Fiber mass fractions of 5, 10, 15, and 20 wt.% were considered in order to assess the influence of reinforcement content on the tensile properties and overall mechanical performance of the developed composites.

Finite element analysis was used to simulate the tensile response of the developed composites and compare the numerical predictions with experimental results. The originality of this work lies in the combined experimental–numerical assessment of untreated Tunisian DPF-reinforced epoxy composites and the evaluation of their potential as sustainable lightweight materials derived from agricultural waste. This approach is aligned with several United Nations Sustainable Development Goals (UNSDGs), particularly responsible consumption and production (SDG 12), industry innovation and infrastructure (SDG 9), and climate action (SDG 13) [18].

2. Theoretical Framework and Modeling of Bio-Composites

2.1. Analytic Modeling of Mechanical Properties

A micromechanical approach can be used to estimate the macroscopic properties of epoxy/palm fiber bio-composites. It is based on the analysis of a representative volume element (RVE) that captures the statistical distribution of microstructures (fibers, matrix, interface). This RVE allows the mechanical behavior to be homogenized based on the properties of the constituents (density, modulus of elasticity, etc.) [15,16].

The effective modulus of elasticity, E_c , can be estimated using Equation (1) :

$$E_c=\eta V_f E_f+V_m E_m \tag{1}$$

Where:

V_f and V_m : volume fractions of the fiber and matrix, respectively, E_f and E_m : elastic moduli of the fiber and matrix constituents, and η : orientation factor.

FEA is essential for validating experimental results, reproducing realistic scenarios based on geometry, fiber arrangement, and fiber-matrix interactions, and refining predictive models [17]. For short-fiber composites, the Kelly-Tyson model is suitable for predicting tensile strength σ_c is presented according to Equation (2):

$$\sigma_c=V_f\,\tau\left(\frac{1}{d}\right)+V_m\sigma_m. \tag{2}$$

Where:

τ: Interfacial shear strength between the fiber and the matrix, $\left(\frac{1}{d}\right)$: Height-to-width ratio of the fibers, and σ_m: Tensile strength of the matrix.

This model is particularly applicable to date palm fiber composites because of the use of short, discontinuous fibers[16].

For composites with randomly oriented short fibers, the Halpin–Tsai model provides a more accurate prediction of the effective modulus:

$$E_c=E_m\left(\frac{1+\zeta\,\eta\,V_f}{1-\eta\,V_f}\right). \tag{3}$$

With:

$$\eta=\frac{\frac{E_f}{E_m}-1}{\frac{E_f}{E_m}+\zeta}. \tag{4}$$

Where:

ζ: Form factor dependent on fiber geometry (for aligned short fibers, 2) , E_c, E_f and E_m: Composite, fiber, and matrix moduli, and V_f : Volume fraction of fibers. This model can better account for the reinforcing efficiency of short natural fibers in the epoxy matrix[19].

The mechanical behavior of the composite specimen under uniaxial tensile loading is studied using the finite element method (FEM), postulating a simplified modeling. The specimen is assumed to behave as a linear elastic isotropic solid under small deformation conditions. This theoretical framework is governed by three fundamental relations of the continuous domain, which are discretized into an algebraic system. First, the Static Equilibrium Equation[19,20]:

$$\nabla \cdot \sigma = 0. \tag{5}$$

Where ∇ is the stress tensor σ, ensuring that the system is in equilibrium under the applied load, neglecting the volumetric forces. Secondly, Hooke's law is expressed as:

$$[\sigma] = [C] \cdot \{\varepsilon\}. \tag{6}$$

Using Equation (6) relates stress (σ) to strain (ε) via the elasticity tensor C, which is entirely determined by Young's modulus (E) and Poisson's ratio (ν). Finally, the strain–displacement relationship is expressed as:

$$\varepsilon = \frac{1}{2}\left(\nabla u + \nabla u^T\right). \tag{7}$$

The solution of the mechanical problem is obtained through discretization of the continuous domain into a finite element system, in accordance with the principle of virtual work. According to this principle, for a body in equilibrium, the virtual work of internal forces equals to the virtual work of external forces[20] :

$$\int_\Omega \delta\varepsilon^T \sigma d\Omega = \int_\Gamma \delta u^T t d\Gamma. \tag{8}$$

The weak formulation of the problem enables the introduction of finite element discretization. By substituting the strain field (ε) using Equation (9):

$$\varepsilon = B \cdot u. \tag{9}$$

Where B is the strain–displacement matrix derived from the interpolation functions and by integrating Hooke's law $\sigma=C\varepsilon$, the governing equation is transformed into the following algebraic matrix system:

$$KU = F. \tag{10}$$

The elementary stiffness matrix K_e is then defined by the following integral :

$$K_e = \int_{\Omega_e} B^T C\, B\, d\Omega. \tag{11}$$

Where:

C is the elasticity tensor dependent on E and ν. The construction of the matrix K_e requires accurate numerical integration, generally performed by Gaussian quadrature, to calculate the vector of nodal displacements U of the assembled system. For three-dimensional isotropic materials, the elasticity matrix C is expressed as[20] :

$$C=\frac{E}{(1+\nu)(1-2\nu)}\begin{bmatrix} 1-\nu & \nu & \nu & 0 \\ \nu & 1-\nu & \nu & 0 \\ \nu & \nu & 1-\nu & 0 \\ 0 & 0 & 0 & \frac{1-2\nu}{2} \\ 0 & 0 & 0 & 0 \\ 0 & 0 & 0 & 0 \end{bmatrix}. \tag{12}$$

2.2. Numerical Validation Indicators

To assess the agreement between the finite element predictions and the experimental measurements, several statistical indicators were considered. The comparison was based on three complementary metrics: the Mean Absolute Percentage Error (MAPE), which expresses the relative deviation between predicted and measured values; the Root Mean Square Error (RMSE), commonly used to evaluate the magnitude of prediction errors; and the coefficient of determination (R^2), which reflects the strength of the correlation between numerical and experimental datasets.

Among these indicators, MAPE provides a direct measure of the percentage difference between the simulated and experimental responses. Lower MAPE values indicate better agreement between the two approaches. The MAPE was determined according to Equation (13):

$$\text{MPAE} = \frac{1}{\text{n}}\sum\nolimits_{\text{i}=1}^{\text{n}}\left|\frac{\sigma_{\text{exp},i} - \sigma_{\text{sim},i}}{\sigma_{\text{exp},i}}\right| * 100. \qquad (13)$$

$\sigma_{\text{exp,i}}$: Experimental stress, $\sigma_{\text{sim,i}}$: Simulated stress, and n: number of data points.

The RMSE was employed to evaluate the global deviation between the numerical and experimental results. The RMSE is expressed by Equation (14):

$$\text{RMSE} = \sqrt{\frac{1}{\text{n}}\sum\nolimits_{\text{i}=1}^{\text{n}}\left(\sigma_{\text{exp,i}}-\sigma_{\text{sim,i}}\right)^2}. \qquad (14)$$

This indicator provides the overall deviation between simulated and experimental results in terms of stress or strain [21]. The coefficient of determination (R^2) was also calculated to assess the quality of the correlation between the experimental and numerical data. The corresponding expression is presented in Equation (15):

$$\text{R}^2=1-\frac{\sum_{\text{i}=1}^{\text{n}}\left(\left(\sigma_{\text{exp,i}}-\sigma_{\text{sim,i}}\right)^2\right.}{\sum_{\text{i}=1}^{\text{n}}\left(\left(\sigma_{\text{exp,i}}-\overline{\sigma_{\text{exp}}}\right)^2\right.}. \qquad (15)$$

3. Materials and Methods

3.1. Raw Materials

The reinforcement fibers investigated in this work were obtained from agricultural residues generated by date palm cultivation in the Tozeur oasis region of southern Tunisia (**Figure 1**). These residues consist primarily of date palm leaf fibers (Lif) derived from *Phoenix dactylifera* L. and represent an abundant lignocellulosic resource that is often discarded or subjected to open-air burning. Such practices not only lead to the loss of potentially valuable biomass but may also contribute to local environmental issues. The use of these by-products as reinforcement materials offers an attractive route for agricultural waste valorization while supporting the replacement of conventional synthetic fibers with renewable alternatives. Owing to its extensive palm plantations and significant annual biomass production, southern Tunisia constitutes a sustainable source of natural fibers suitable for composite applications.

The polymer matrix selected for this study was a commercial thermosetting epoxy resin supplied by DORMAN and used in combination with its corresponding hardener. The resin is based on a diglycidyl ether of bisphenol A (DGEBA) system, a formulation frequently adopted in composite manufacturing because of its reliable processing behavior, good mechanical performance, and favorable adhesion with reinforcing fibers. These characteristics make epoxy resins particularly suitable for the development of structural and semi-structural bio-composites.

Date palm fibers were used as reinforcement material, while the epoxy resin served as the continuous matrix phase of the developed bio-composites. According to the manufacturer's technical datasheet, the epoxy resin exhibits a density of approximately 1.10 g/cm^3, a Young's modulus close to 2 GPa, and an elongation at break of about 1.5%.

Figure 1. Raw date palm fibers collected from agricultural waste in the Tozeur oasis region (southern Tunisia).

In the present work, epoxy/date palm fiber bio-composites with different fiber mass fractions (5, 10, 15, and 20 wt%) were manufactured and experimentally investigated under tensile loading conditions. The main objective of this study is to evaluate the influence of fiber content on the tensile behavior of the developed bio-composites through the determination of Young's modulus (E), maximum tensile stress σ_{max} , and strain at failure ε_{max} .

3.2. Manufacturing Process

The bio-composite specimens were manufactured using a manual molding technique because of its simplicity, low cost, and suitability for thermosetting composites at the laboratory scale. The date palm fiber powder was gradually added to the epoxy resin and manually stirred until a uniform dispersion of the reinforcement within the matrix was achieved.

The resulting mixture was subsequently cast into flat molds previously lined with silicone membranes to facilitate specimen removal after curing. To improve composite quality, manual consolidation was carried out using a roller laminator. This operation helped minimize air entrapment within the material and promoted more effective wetting and impregnation of the date palm fibers by the epoxy resin.

After molding, the composite plates were cured in an oven at temperatures between 30 and 40 °C for approximately 20 h to ensure proper polymerization of the epoxy system. The cured specimens were subsequently demolded and stored under ambient conditions prior to mechanical testing. **Figure 2** illustrates the manufacturing process, from the extraction of the fibre to the development of the bio-composite tensile samples.

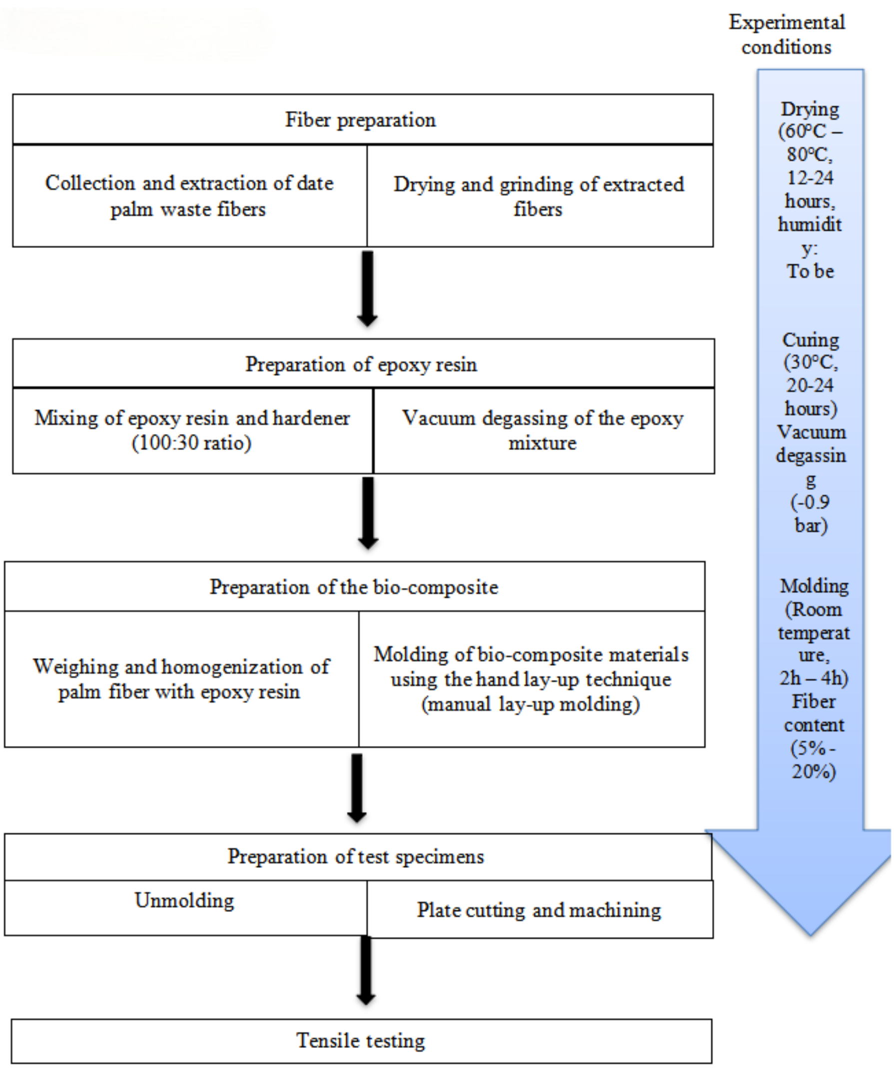

Figure 2. Manufacturing and testing process.

3.3. Physical Properties and Void Content Analysis

The theoretical density ρ_{th} of the composite can be calculated from the weight fractions and densities of its constituents by using Equation (16)[22]:

$$\frac{1}{\rho_{th}} = \frac{w_f}{\rho_f} + \frac{w_m}{\rho_m}. \tag{16}$$

Where: w_f , w_m : Weight fractions of fibers and matrix and ρ_f , ρ_m : Densities of the fiber and matrix

The void content, which affects mechanical performance, is calculated as follows:

$$\text{Void content}(\%) = \left(\frac{\rho_{th} - \rho_{exp}}{\rho_{th}}\right) * 100. \tag{17}$$

Void content is an important indicator of impregnation quality and manufacturing defects in composite materials[22].

3.4. Experimental Conditions

The epoxy/date palm fiber bio-composites were fabricated under controlled processing conditions in order to ensure repeatability and consistent specimen quality. The process involved adjusting the mass fraction of the fibers (5%, 10%, 15%, and 20%), which is essential for determining the final properties of the material. Other factors, such as the temperature and duration of the epoxy resin curing, as well as the cooling time of the composite plate, were precisely managed to ensure the quality and structural integrity of the product, as indicated in **Table 1** of experimental parameters.

Once preparation was complete, mechanical characterization was performed using a tensile test, which evaluated the performance of the bio-composite by measuring the tensile force applied until breakage. The adopted manufacturing procedure ensured good control of fiber distribution and specimen preparation before tensile characterization, making it possible to directly link the manufacturing conditions to the mechanical properties of the material, as indicated in **Table 2** of the sample composition.

The fiber mass fraction was limited to 20 wt.% in the present study in order to maintain acceptable processability, homogeneous mixing, and adequate impregnation of the epoxy matrix during manual molding. Preliminary fabrication trials indicated that higher fiber contents significantly increased mixture viscosity and promoted fiber agglomeration and void formation, which may negatively affect specimen quality and mechanical reproducibility

Table 1. Experimental parameters taken into account for the development of the new bio-composite.

Settings	Description	Range
T (°C)	Test temperature	30
DPF (%)	Percentage of palm fiber in the bio-composite	5–10–15–20
t (hour)	Epoxy resin curing time	12–14 h
D (hour)	Cooling time of the bio-composite plate	24 h
F (N)	Traction force of experimental tests	11–316 N

Table 2. Sample composition.

Samples	PF (w%)	Composition	Prepared Samples
1	5%	Epoxy resin + 5% PF	
2	10%	Epoxy resin + 10% PF	
3	15%	Epoxy resin + 15% PF	
4	20%	Epoxy resin + 20% PF	

3.5. Mechanical Characterization

Tensile tests were conducted following the general recommendations of ASTM D3039 for polymer matrix composites and ISO 527-2/ASTM D638 standards for reinforced plastic materials, while adapting the specimen dimensions to the manufacturing constraints associated with the manually fabricated bio-composite plates.

The test specimens had a rectangular geometry with nominal dimensions of 100 × 25 × 5 mm. The total specimen length was reduced compared to the standard ASTM D3039 geometry in order to optimize material utilization and ensure fabrication consistency. The adopted dimensions are comparable to ISO 527-2 type 1B or ASTM D638 type IV specimen geometries while maintaining acceptable geometric proportions between gauge length and specimen width.

To minimize gripping-induced damage and stress concentration effects, fiberglass tabs were bonded at both specimen ends prior to testing. Axial deformation was measured using a clip-on extensometer with a gauge length of 25 mm. The tensile tests were performed under controlled conditions of machine alignment, grip pressure, and crosshead displacement rate in accordance with the recommendations of the selected testing standards. The geometry of the tensile specimen is illustrated in **Figure 3**.

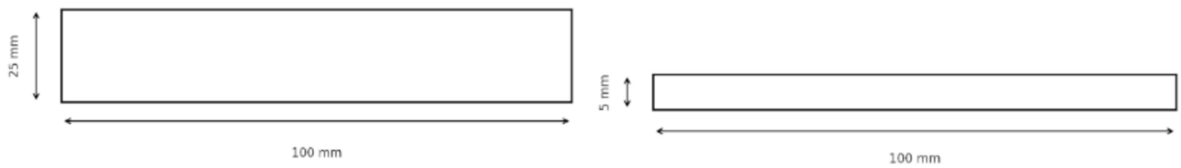

Figure 3. Geometry and dimensions of the tensile test specimen used in this study (100 mm × 25 mm × 5 mm).

4. Experimental Results and Discussion

4.1. Tensile Stress–Strain Behavior

This section presents the tensile test results obtained for the developed epoxy/date palm fiber bio-composites reinforced with date palm fibers, highlighting the influence of the fiber mass fraction (5, 10, 15, and 20%) on the mechanical properties under tension. The investigated properties included maximum stress σ_{max} , elongation at break (ε), and modulus of elasticity (E). **Figure 4** presents the experimental stress–strain curves obtained from tensile testing of epoxy/date palm fiber bio-composites with different fiber mass fractions.

Figure 5 presents a representative tensile test and the corresponding fractured specimen after failure. The fracture occurred within the gauge section of the specimen, indicating that the applied loading conditions were appropriate and that no premature failure occurred near the grips. The observed fracture mode is consistent with the tensile behavior of short natural fiber-reinforced composites.

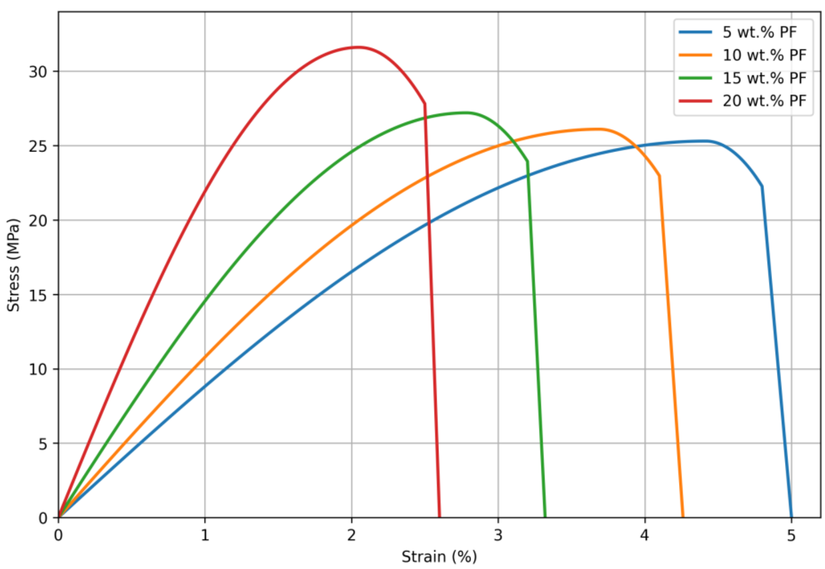

Figure 4. Experimental stress-strain curves for tensile testing of the epoxy-palm fiber bio-composite for different fiber mass fractions (5%, 10%, 15%, and 20%).

(a) (b)

Figure 5. Tensile testing and failure of the epoxy/date palm fiber bio-composites: (**a**) Specimen during tensile testing; (**b**) Representative fractured specimen after tensile testing.

4.2. Conversion of Load–Displacement Data into Stress–Strain Curves

The tensile testing machine directly records the load–displacement response of each specimen. To enable comparison between formulations and determine the mechanical properties of the developed bio-composites, the experimental data were converted into engineering stress–strain curves.

The engineering stress was calculated using Equation (18)[23]:

$$\sigma = \frac{F}{A_0}. \tag{18}$$

Where F is the applied load and A_0 is the initial cross-sectional area of the specimen.

The engineering strain was determined using Equation (19)[23]:

$$\varepsilon = \frac{\Delta L}{L_0}. \tag{19}$$

Where ΔL is the measured displacement and L_0 is the initial gauge length.

Since the original tensile testing machine records load and displacement during testing, the engineering stress–strain curves were obtained using Equations (18) and (19). To illustrate this conversion procedure, representative load–displacement responses were reconstructed from the experimentally measured tensile properties. These reconstructed curves are provided for visualization purposes and remain consistent with the experimentally measured stiffness, tensile strength, and elongation at break of the investigated formulations, as illustrated in **Figure 6**.

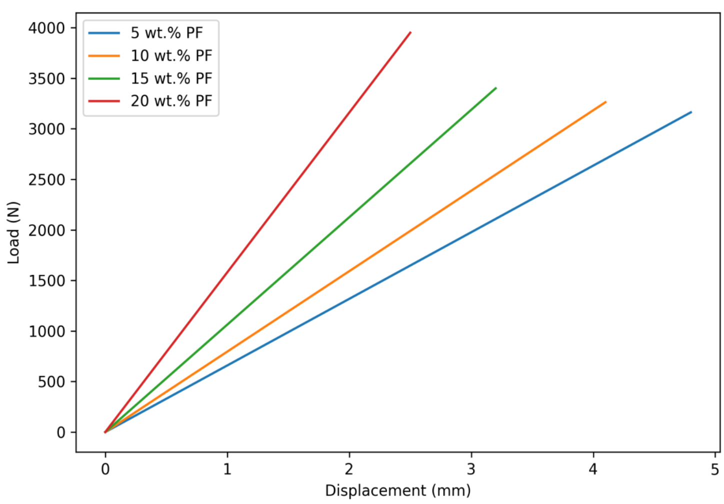

Figure 6. Representative reconstructed load–displacement curves derived from the experimentally measured tensile properties of the epoxy/date palm fiber bio-composites.

4.3. Evolution of Mechanical Properties

Table 3 summarizes the tensile properties of the epoxy/date palm fiber bio-composites for different fiber mass fractions (5–20 wt%). In accordance with ASTM D3039, five specimens were tested for each five mass fraction.

As indicated in **Table 3**, the density of the composites increased slightly from 1.15 to 1.25 g/cm^3 with increasing fiber content, remaining consistent with the density range commonly reported for epoxy-based natural fiber composites.

The experimental results reveal that increasing the date palm fiber content progressively improves the tensile strength and stiffness of the developed bio-composites. The maximum tensile stress increased from 25.3 MPa at 5 wt.% fiber loading to 31.6 MPa at 20 wt.%, while the Young's modulus increased from 2.00 GPa to 3.67 GPa. This behavior can be attributed to the reinforcing effect of the lignocellulosic fibers, which enhance stress transfer within the epoxy matrix and restrict polymer chain mobility.

Conversely, the elongation at break decreased from 4.8% to 2.5% as the fiber loading increased, indicating a progressive reduction in ductility and a transition toward a stiffer mechanical response. The intermediate formulations containing 10 wt% and 15 wt% fibers exhibited balanced tensile behavior, combining moderate stiffness with acceptable deformation capacity.

Overall, the results suggest that untreated date palm fibers can improve the stiffness and tensile resistance of the epoxy matrix while reducing its deformability. Among the investigated formulations, the composites containing 15–20 wt% fibers exhibited the most favorable compromise between tensile performance and structural stiffness.

The observed increase in tensile stiffness with increasing fiber loading is consistent with trends reported for other natural fiber-reinforced epoxy composites, such as sisal, jute, and flax systems, reported in the literature. Similar reductions in elongation at break were also observed in lignocellulosic bio-composites due to the progressive restriction of matrix deformation caused by rigid fiber incorporation. However, the absolute tensile properties obtained in the present study remain dependent on several factors, including fiber treatment, fiber dispersion, interfacial adhesion, and manufacturing conditions.

Table 3. Mechanical properties of epoxy/palm fiber bio-composite for different fiber mass fractions (5%, 10%, 15%, and 20%).

Samples	PF (w%)	n	ρ(g/cm^3)	σ_{max} (MPa)	ε_{max}(%)	E (GPa)
1	5%	5	1.15	25.3 ± 0.63	4.8 ± 1.1	2 ± 0.12
2	10%	5	1.18	26.1 ± 0.74	4.1 ± 0.9	2.55 ± 0.11
3	15%	5	1.21	27.2 ± 0.79	3.2 ± 0.7	3.1 ± 0.17
4	20%	5	1.25	31.6 ± 1.10	2.5 ± 0.5	3.67 ± 0.25

4.4. Discussion of the Reinforcement Effect

In addition to the macroscopic mechanical behavior, the evolution of the tensile properties may also be influenced by the quality of the fiber–matrix interactions within the composite structure. The progressive increase in tensile strength and stiffness with increasing fiber content suggests an improved stress transfer capability between the epoxy matrix and the date palm fibers. The decrease in elongation at break observed with increasing fiber content suggests a progressive shift toward a more rigid material response accompanied by reduced ductility.

It should be noted that no microstructural characterization was carried out in the present work. As a result, mechanisms occurring at the microscopic scale, including fiber–matrix interfacial interactions, fiber pull-out, matrix cracking, and damage initiation, could not be examined directly. Consequently, the discussion of the reinforcement mechanisms is mainly derived from the macroscopic tensile behavior and the evolution of the measured mechanical properties.

A more detailed understanding of the deformation and failure processes could be achieved through complementary microstructural investigations. In particular, scanning electron microscopy (SEM) of fractured specimens would provide valuable information regarding interfacial bonding quality, void content, crack propagation paths, and fracture morphology, thereby offering deeper insight into the mechanisms controlling the tensile performance of the developed bio-composites.

5. Numerical Modeling and Simulation

5.1. Finite Element Implementation

Finite element simulations were performed using the static structural module of ANSYS Workbench in order to evaluate the global tensile behavior of the developed epoxy/date palm fiber bio-composites. The geometry of the numerical model was defined according to the experimental tensile specimen dimensions (100 mm × 25 mm × 5 mm), ensuring consistency between the experimental and numerical approaches.

In the present study, the bio-composite was modeled as an equivalent homogenized isotropic material using experimentally determined effective mechanical properties for each fiber mass fraction (5, 10, 15, and 20 wt%). This simplified homogenized approach was adopted to investigate the overall tensile response of the composite at the macroscopic scale. The experimentally measured Young's modulus and density values were directly integrated into the finite element material database, while a constant Poisson's ratio of 0.35 was assumed for all formulations based on values commonly reported for epoxy-based natural fiber composites.

One end of the specimen was fully constrained, whereas a uniaxial tensile displacement was applied at the opposite end in order to reproduce the experimental tensile loading conditions. The numerical simulations were performed under simplified linear elastic assumptions. Consequently, the present numerical model should be considered as a first-order approximation of the global tensile response rather than a full representation of the nonlinear deformation behavior observed experimentally.

The objective of the finite element analysis was not to reproduce the local heterogeneous microstructure of the composite or the fiber/matrix interface behavior, but rather to provide a simplified macroscopic representation capable of comparing the global evolution of tensile stiffness and stress distribution as a function of fiber content (**Table 4**).

Table 4. Mechanical properties integrated into the finite element model for different fiber mass fractions.

PF (wt.%)	Density (g/cm^3)	Young's Modulus (GPa)	Poisson's Ratio
5	1.15	2	0.35
10	1.18	2.55	0.35
15	1.21	3.10	0.35
20	1.25	3.67	0.35

The developed numerical model enabled the comparison between experimental and simulated tensile responses for the different reinforcement contents. Although the adopted homogenized isotropic approach does not explicitly account for local fiber distribution, interfacial effects, or damage evolution mechanisms, it provides a first-order approximation of the global mechanical behavior of the developed bio-composites under tensile loading.

It should be noted that the micromechanical and analytical models introduced in this study were not directly implemented within ANSYS through user-defined constitutive laws, customized material subroutines, or multiscale coupling procedures. Instead, these theoretical formulations were employed to interpret the influence of fiber content on the effective mechanical properties of the developed bio-composites.

For the finite element simulations, a homogenized linear-elastic isotropic material model was adopted. The experimentally determined Young's modulus values corresponding to each fiber mass fraction were directly assigned as material properties in the ANSYS database, while the density values were also incorporated into the numerical model. Consequently, the finite element simulations describe the macroscopic tensile response of the composite rather than the local fiber–matrix interactions and damage mechanisms governing the material behavior at the microscale.

Therefore, the analytical models and finite element simulations should be considered complementary approaches. The former provide a theoretical interpretation of the reinforcement mechanisms associated with increasing fiber content, whereas the latter evaluate the global stress distribution, deformation field, and stiffness evolution at the structural scale. This combined methodology provides both a mechanistic understanding of the material behavior and a numerical assessment of its macroscopic response under tensile loading.

5.2. Finite Element Boundary Conditions and Mesh Generation

The tensile response of the developed bio-composites was simulated using the finite element method under static loading conditions. The numerical model reproduced the geometry of the experimental tensile specimen with dimensions of 100 mm × 25 mm × 5 mm.

To reproduce the experimental tensile test conditions, one end of the specimen was fully constrained, while a uniaxial tensile displacement was applied at the opposite end, in accordance with the ASTM D3039 tensile loading configuration. These conditions reproduced the global tensile loading configuration used experimentally.

The finite element mesh was generated automatically using three-dimensional volumetric solid elements. A mesh sensitivity analysis was carried out in order to obtain a suitable compromise between numerical accuracy and computational efficiency. The final mesh configuration was selected after verifying the stability of the numerical results with mesh refinement (**Figure 7**).

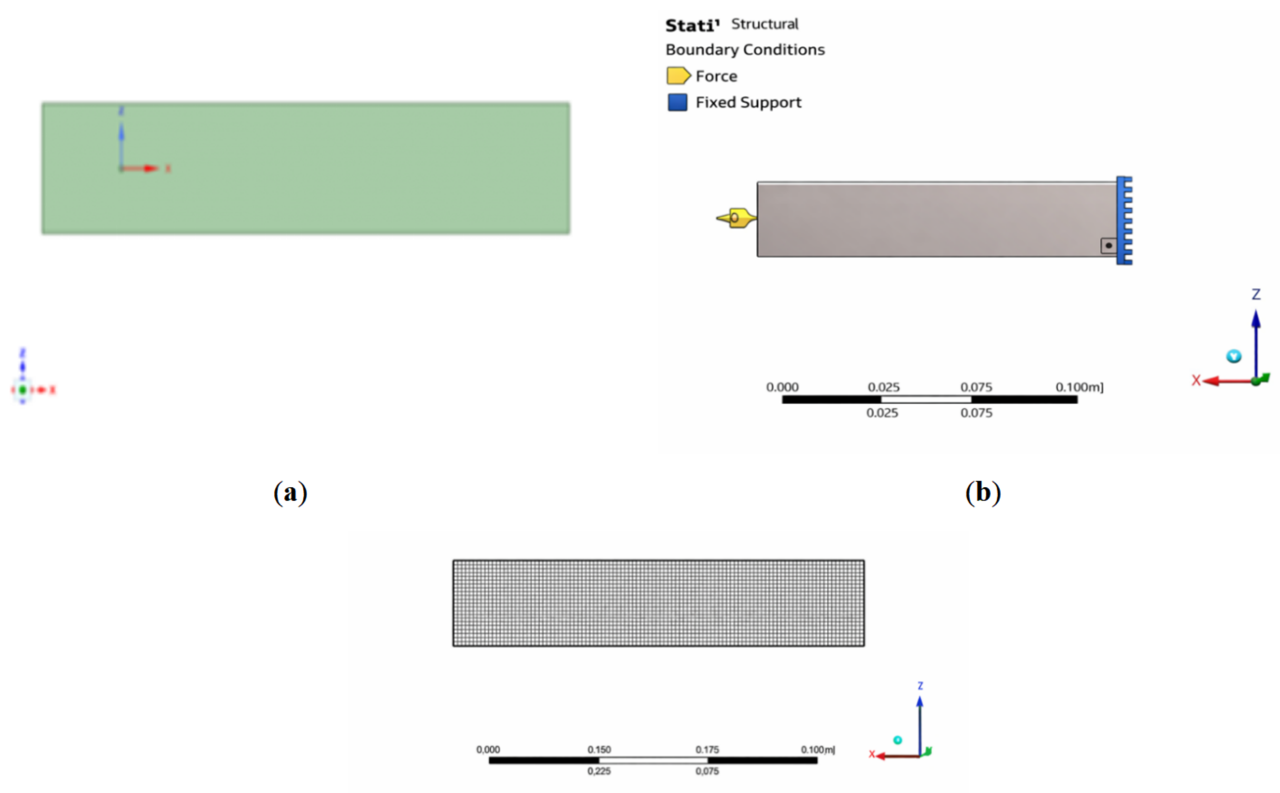

(a) (b) (c)

Figure 7. (**a**) Geometry of the test specimen modeled; (**b**) Boundary conditions and loading; (**c**) Mesh of the test specimen.

5.3. Mesh Convergence and Numerical Validation

Prior to the numerical simulations, a mesh convergence study was conducted to ensure the numerical stability of the finite element model.

Several mesh densities were investigated, and the resulting maximum stress values were monitored. The predicted stresses became nearly independent of mesh refinement beyond approximately 6,000 elements, indicating satisfactory convergence, as indicated in **Table 5**. The final mesh was therefore selected as a compromise between computational efficiency and numerical accuracy.

Table 5. Mesh convergence study.

Number of Elements	Maximum Stress (MPa)	Relative Error (%)
1,500	30.2	4.4
3,000	31.0	1.9
6,000	31.5	0.3
12,000	31.6	0.0

Note: The convergence study was performed using the 20 wt.% formulation because it generated the highest stress level and therefore represents the most demanding numerical configuration.

5.4. Numerical Model Calibration and Validation

To assess the reliability of the finite element model, the numerical predictions were compared with the experimental tensile results obtained for the four fiber mass fractions. The calibration procedure consisted of assigning the experimentally measured Young's modulus values to the homogenized isotropic material model implemented in ANSYS. The numerical tensile response was then evaluated and compared with the corresponding experimental measurements.

The comparison showed good agreement between numerical and experimental results, particularly for fiber contents between 5 wt.% and 15 wt.%, where the prediction errors remained below 8%. Larger deviations were observed for the 20 wt.% formulation due to the increasing influence of fiber agglomeration, local heterogeneity, and interfacial effects that are not explicitly represented by the simplified homogenized model.

Overall, the obtained correlation confirms that the developed finite element model is capable of reproducing the global tensile behavior of the investigated bio-composites and can therefore be used as a reliable first-order engineering approximation.

5.5. Experimental–Numerical Load–Displacement Comparison

To further assess the reliability of the developed finite element model, the tensile load–displacement responses obtained experimentally were compared with the corresponding numerical predictions. The finite element simulations were performed under displacement-controlled loading conditions reproducing the experimental tensile tests. Representative load–displacement curves for the investigated fiber mass fractions are presented in **Figure 8**.

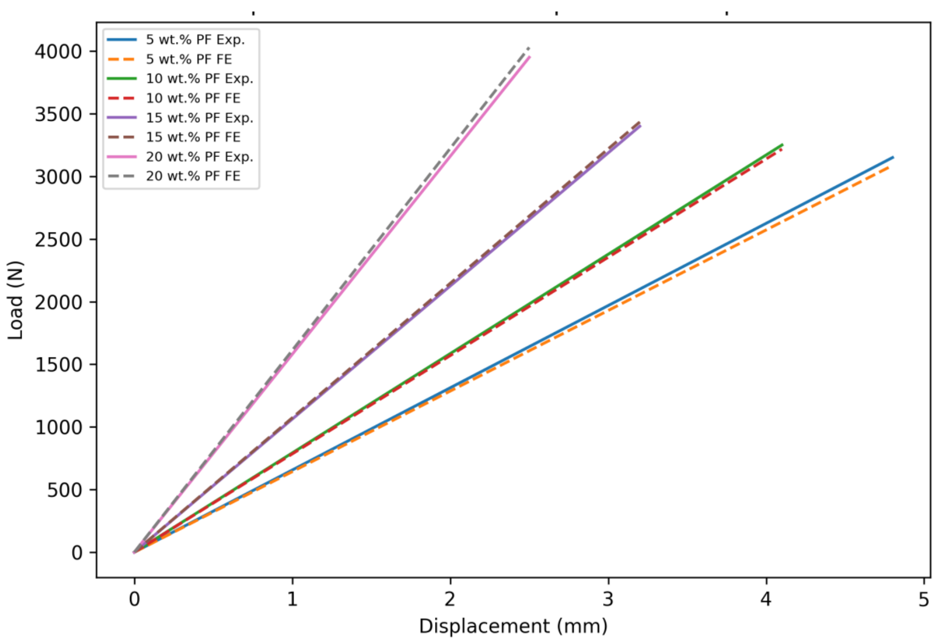

Figure 8. Comparison between experimental and finite element load–displacement responses of epoxy/date palm fiber bio-composites for different fiber mass fractions.

A satisfactory agreement was observed between the experimental and numerical responses for all formulations. The finite element model successfully reproduced the overall stiffness evolution associated with the increase in fiber content. Minor discrepancies observed at high fiber fractions can be attributed to local material heterogeneity, fiber agglomeration, void formation, and fiber–matrix interfacial effects that are not explicitly represented in the adopted homogenized linear elastic model.

These results confirm that the developed finite element approach provides a reliable first-order approximation of the global tensile behavior of the epoxy/date palm fiber bio-composites.

5.6. Finite Element Simulation Results

The numerical simulation results, illustrated in **Figure 9**, show the distribution of maximum stresses in the epoxy/palm fiber bio-composite for different fiber mass fractions (5%, 10%, 15%, and 20%).

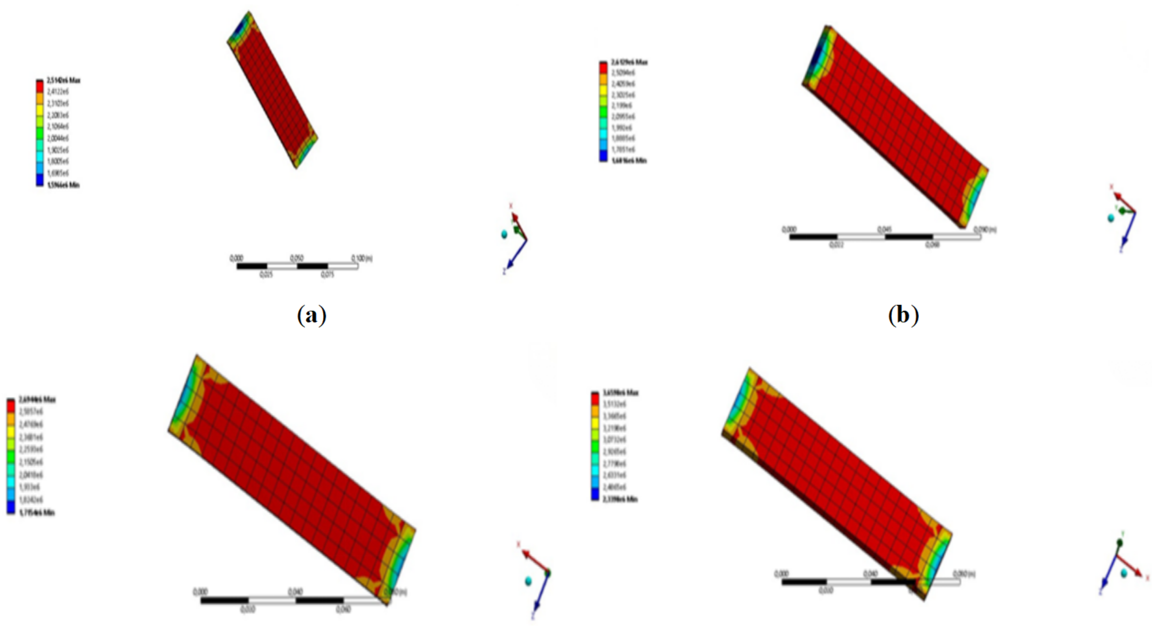

Figure 9. Distribution of simulated maximum stresses in palm fiber-reinforced epoxy bio-composite for different fiber contents: (**a**) 5%; (**b**) 10%; (**c**) 15%; (**d**) 20%.

Finite element simulations were performed to analyze the global stress distribution within the epoxy/date palm fiber bio-composite specimens for different fiber mass fractions (5, 10, 15, and 20 wt%). The numerical results provide complementary information to the experimental tensile tests by illustrating the evolution of the stress fields under tensile loading conditions.

Figure 6 presents the simulated equivalent stress distributions obtained for the different composite formulations. For all fiber contents, higher stress levels are mainly observed near the constrained and loaded regions of the specimen, which is consistent with the applied boundary conditions and tensile loading configuration.

The increase in fiber content resulted in higher global stiffness values in the numerical model due to the experimentally measured increase in Young's modulus integrated into the finite element simulations. Consequently, the specimens reinforced with 15 wt% and 20 wt% fibers exhibited higher stress levels and lower overall deformation compared with lower fiber fractions. These numerical observations are consistent with the experimental tensile results, which showed an increase in tensile strength and stiffness with increasing fiber content. It should be noted that the present finite element model was developed using a simplified homogenized linear elastic isotropic approach. Therefore, the simulations represent the macroscopic global mechanical response of the composite and do not explicitly capture the heterogeneous microstructure, local fiber–matrix interactions, interfacial stress concentrations, or damage evolution mechanisms occurring at the microscopic scale. The consistency between the finite element predictions and the experimental measurements was assessed using the MAPE, RMSE, and coefficient of determination (R^2) indicators. The obtained results revealed a satisfactory level of agreement for all investigated formulations, with the closest correspondence observed for composites containing low and intermediate fiber contents. The larger discrepancies identified at higher reinforcement levels are likely related to factors that were not explicitly represented in the numerical model, including local material heterogeneity, non-uniform fiber distribution, void formation, and variability in fiber–matrix interactions.

Despite these limitations, the developed finite element model successfully captured the overall trends observed during tensile testing. The numerical approach therefore constitutes a reliable tool for describing the global mechanical response of the epoxy/date palm fiber composites and for evaluating the effect of reinforcement content on their tensile behavior at the macroscopic scale.

6. Evaluation of Discrepancies between Experimental and Numerical Results

To evaluate the capability of the developed finite element model to reproduce the global tensile behavior of the epoxy/date palm fiber bio-composites, a comparison between experimental measurements and numerical predictions was carried out. The comparison focused on the maximum tensile stress σ_{max} and the maximum strain ε_{max} obtained for different fiber mass fractions.

The prediction accuracy of the numerical model was assessed using the MAPE, the RMSE, and the coefficient of determination (R^2). These indicators provide quantitative information regarding the deviation between experimental and numerical results (**Tables 6** and **7**).

Table 6. Evaluation of discrepancies between experimental and numerical results for σ_{max} and ε_{max} at different PF percentages, based on MPAE and RMSE indicators.

	PF	Experimental Results	Numerical Results	MPAE (%)	RMSE
σ_{max} (MPa)	5%	25.3 ± 0.63	25.1	0.79	0.20
	10%	26.1 ± 0.74	26.1	0.00	0.00
	15%	27.2 ± 0.79	26.9	1.10	0.30
	20%	31.6 ± 1.10	36.6	15.82	3.5
ε_{max} (%)	5%	4.8 ± 1.1	4.5	6.25	0.30
	10%	4.1 ± 0.9	3.8	7.31	0.30
	15%	3.2 ± 0.7	3	6.25	0.20
	20%	2.5 ± 0.5	2.1	16	0.40

Table 7. Comparison of numerical prediction accuracy with previous studies on natural fiber composites.

Reference	Composite Material	Numerical Approach	Accuracy Indicator	Reported Value
Present study	Epoxy/date palm fiber	Homogenized linear elastic FEM	R^2 (σ_{max})	0.979
Present study	Epoxy/date palm fiber	Homogenized linear elastic FEM	R^2 (ε_{max})	0.994
Present study	Epoxy/date palm fiber	Homogenized linear elastic FEM	MAPE	0–16%
Betelie et al. [24]	Sisal fiber/epoxy composite	FEM tensile simulation	Relative error	5–12%
Covallane et al. [25]	Jute fiber composite	Experimental–numerical comparison	Prediction error	5–15%
Rafiquzzaman et al. [26]	Bio-based composite	FEM coupled modeling	R^2	0.91–0.97

The comparison between experimental and numerical results showed acceptable agreement at the macroscopic scale for the developed epoxy/date palm fiber bio-composites. The numerical model provided coefficients of determination (R^2) of approximately 0.979 for the maximum tensile stress and 0.994 for the maximum strain, indicating a strong correlation between experimental measurements and numerical predictions. In addition, the MAPE values remained relatively low for fiber contents between 5 wt% and 15 wt%, whereas larger deviations were observed for the 20 wt.% formulation.

Table 5 compares the prediction accuracy of the present numerical approach with previous studies reported in the literature on natural fiber-reinforced composites. Similar predictive performances were reported for sisal fiber/epoxy composites, with relative errors ranging from 5% to 12%[24]. Likewise, simulations conducted on jute fiber composites showed prediction errors between 5% and 15% depending on fiber content and interfacial conditions[25]. More recent investigations on bio-based composites reported coefficients of determination ranging from 0.91 to 0.97 for tensile property prediction[26].

The larger discrepancies observed at high fiber contents in the present work may be associated with increased material heterogeneity, local fiber agglomeration, void distribution, and interfacial effects that are not fully captured by the simplified homogenized isotropic finite element model. Nevertheless, despite the simplifying assumptions adopted in the present linear elastic FEM approach, the numerical simulations provide a reasonable first-order macroscopic approximation of the experimental tensile behavior of the developed bio-composites. However, these correlations mainly reflect the capability of the homogenized model to reproduce the overall trends of the tensile response rather than the localized heterogeneous behavior of the composite material.

7. Conclusions

This study investigated the tensile behavior of epoxy bio-composites reinforced with untreated DPFs collected from southern Tunisia using through experimental tensile testing and FEA. The results demonstrated that increasing the fiber mass fraction enhanced the tensile performance and stiffness of the developed composites. The maximum tensile stress increased from 25.3 MPa at 5 wt% fiber content to 31.6 MPa at 20 wt% fiber content, while the Young's modulus increased from 2.0 GPa to 3.67 GPa. Conversely, the strain at failure decreased from 4.8% to 2.5%, indicating a progressive transition toward stiffer and less ductile mechanical behavior with increasing fiber reinforcement.

Finite element simulations were carried out using a homogenized linear elastic isotropic representation of the developed bio-composites. At the macroscopic level, the numerical predictions reproduced the main trends observed experimentally. The comparison between both datasets resulted in coefficients of determination (R^2) of approximately 0.979 for tensile strength and 0.994 for maximum strain. The closest agreement was obtained for composites containing low and intermediate fiber fractions, whereas the formulation reinforced with 20 wt.% date palm fibers exhibited larger deviations. Such differences are likely associated with phenomena that were not explicitly incorporated into the numerical model, including local variations in fiber distribution, agglomeration effects, void formation, and the complexity of fiber–matrix interactions.

The combined experimental and numerical investigation highlights the potential of untreated Tunisian date palm fibers as reinforcement materials for lightweight epoxy-based bio-composites. Beyond the mechanical benefits observed in this study, the utilization of these fibers represents an attractive strategy for converting agricultural residues into value-added engineering materials. The developed composites may therefore be considered for applications requiring moderate mechanical performance together with reduced environmental impact, including interior panels, partition systems, insulation components, and other lightweight secondary structures. From a broader perspective, the exploitation of locally available biomass resources may also support sustainable material development and contribute to the economic valorization of agricultural by-products in arid regions.

The scope of the present investigation was restricted to tensile loading under quasi-static conditions. Other aspects that may influence long-term performance, such as moisture uptake, thermal aging, environmental degradation, fatigue loading, impact behavior, and durability, were not addressed. Furthermore, no microstructural examination was conducted to directly assess fracture mechanisms, interfacial bonding quality, or damage development within the composite. The numerical approach was likewise based on a simplified homogenized formulation and did not explicitly represent microstructural heterogeneity, damage progression, or localized stress concentrations.

Additional research would be valuable to further improve the understanding and performance of date palm fiber-reinforced bio-composites. Particular attention could be given to fiber surface modification, optimization of fiber dispersion and orientation, microstructural characterization of fractured specimens, durability studies under service conditions, and the implementation of advanced multi-scale or non-linear numerical approaches capable of describing the complex behavior of natural fiber composite systems with greater accuracy.

Author Contributions

Conceptualization, I.I., L.L. and R.N.; methodology, I.I.; software, I.I.; validation, S.B.K. and R.N.; formal analysis, I.I., A.R., K.E.M. and L.L.; investigation, I.I. and A.R.; resources, K.E.M.; data curation, I.I.; writing—original draft preparation, I.I. and L.L.; writing—review and editing, S.B.K., R.N., A.R. and K.E.M.; visualization, I.I.; supervision, S.B.K. and R.N.; project administration, S.B.K. and R.N. All authors have read and agreed to the published version of the manuscript.

Funding

This research received no external funding.

Institutional Review Board Statement

Not applicable.

Informed Consent Statement

Not applicable.

Data Availability Statement

The data supporting the findings of this study are available from the corresponding author upon reasonable request.

Acknowledgments

The authors would like to acknowledge the technical support provided by the laboratory staff during the experimental work.

Conflicts of Interest

The authors declare no conflict of interest.

AI Use Statement

The authors used Grammarly tools exclusively for grammar correction and improvement of English readability. All experimental work, numerical simulations, data analysis, interpretation of results, and scientific conclusions were conceived and performed solely by the authors. The authors subsequently reviewed and edited the content as necessary and take full responsibility for the final content of the published article.

Abbreviations

MPa	Megapascal
GPa	Gigapascal
%	Percentage
g/cm^3	Grams per cubic centimetre
°C	Degrees Celsius
mm	Millimetre
N	Newton
H	Hour
DPF	Date palm fibers
FEA	Finite element analysis
NFRP	Natural fiber-reinforced polymer composites
RVE	Representative volume element
MAPE	Mean Absolute Percentage Error
RMSE	Root Mean Square Error
ASTM	American Society for Testing and Materials
ISO	International Organization for Standardization
UNSDGs	United Nations Sustainable Development Goals

References

[1] Ramachandran, A., Rangappa, S.M., Kushvaha, V., et al., 2022. Modification of Fibers and Matrices in Natural Fiber Reinforced Polymer Composites: A Comprehensive Review. Macromolecular Rapid Communications. 43(17), 2100862. DOI: https://doi.org/10.1002/marc.202100862

[2] Sanjay, M.R., Siengchin, S., Parameswaranpillai, J., et al., 2019. A comprehensive review of techniques for natural fibers as reinforcement in composites: Preparation, processing and characterization. Carbohydrate Polymers. 207, 108–121. DOI: https://doi.org/10.1016/j.carbpol.2018.11.083

[3] Sanjay, M.R., Madhu, P., Jawaid, M., et al., 2018. Characterization and properties of natural fiber polymer composites: A comprehensive review. Journal of Cleaner Production. 172, 566–581. DOI: https://doi.org/10.1016/j.jclepro.2017.10.101

[4] Ramesh, M., Deepa, C., Kumar, L.R., et al., 2022. Life-cycle and environmental impact assessments on processing of plant fibres and its bio-composites: A critical review. Journal of Industrial Textiles. 51, 5518S. DOI: https://doi.org/10.1177/1528083720924730

[5] Mahmud, M.Z.A., Rabbi, S.M.F., Islam, M.D., et al., 2025. Synthesis and applications of natural fiber-reinforced epoxy composites: A comprehensive review. SPE Polymers. 6(1), e10161. DOI: https://doi.org/10.1002/pls2.10161

[6] Borah, P.P., Kashyap, S., Kirtania, S., et al., 2024. Finite element and numerical analysis for structural responses of natural fibre-based epoxy composites. International Journal on Interactive Design and Manufacturing (IJIDeM). 18(4), 1955–1967. DOI: https://doi.org/10.1007/s12008-022-00915-z

[7] Abass, R.U., Al-Sarraf, M.A., Bachtiar, D., et al., 2024. Eco-friendly mechanical performance of date palm Khestawi-type fiber-reinforced polypropylene composites. Journal of the Mechanical Behavior of Materials. 33(1), 20240019. DOI: https://doi.org/10.1515/jmbm-2024-0019

[8] Islam, S., Karim, F., Islam, M.R., et al., 2025. Thermoset and thermoplastic polymer composite with date palm fiber and its behavior: A review. SPE Polymers. 6(1), e10157. DOI: https://doi.org/10.1002/pls2.10157

[9] Boey, J.Y., Yusoff, S.B., Tay, G.S., 2022. A review on the enhancement of composite's interface properties through biological treatment of natural fibre/lignocellulosic material. Polymers and Polymer Composites. 30. DOI: https://doi.org/10.1177/09673911221103600

[10] Awad, S.A., Jawaid, M., Ismail, A.S., et al., 2024. Dimension stability, tensile and thermomechanical properties of bamboo/oil palm fibre reinforced bio-epoxy hybrid biocomposites. Journal of Materials Research and Technology. 30, 7440–7446. DOI: https://doi.org/10.1016/j.jmrt.2024.05.130

[11] Niu, C., Zhang, Q., Cheng, L., et al., 2023. Microstructure and mechanical properties of Cf/SiC composites with dispersed C-SiC interphase prepared by chemical vapor infiltration. Composites Part A: Applied Science and Manufacturing. 165, 107339. DOI: https://doi.org/10.1016/j.compositesa.2022.107339

[12] Ali, A.E., Abdellah, M.. Y., Gronfula, M., et al., 2025. Reinforcing Polymers with Date Palm Seeds: A Path to Greener Composites—A Review. SVU-International Journal of Engineering Sciences and Applications. 6(2), 1–16. DOI: https://doi.org/10.21608/svusrc.2025.359294.1271

[13] Etale, A., Onyianta, A.J., Turner, S.R., et al., 2023. Cellulose: A Review of Water Interactions, Applications in Composites, and Water Treatment. Chemical Reviews. 123(5), 2016–2048. DOI: https://doi.org/10.1021/acs.chemrev.2c00477

[14] Dehury, J., Mohanty, J.R., Nayak, S., et al., 2022. Comprehensive Characterization of Date Palm Petiole Fiber Reinforced Epoxy Composites: Effect of Fiber Treatment and Loading on Various Properties. Journal of Natural Fibers. 19(14), 9457–9470. DOI: https://doi.org/10.1080/15440478.2021.1982834

[15] Torres-Arellano, M., Renteria-Rodríguez, V., Franco-Urquiza, E., 2020. Mechanical Properties of Natural-Fiber-Reinforced Biobased Epoxy Resins Manufactured by Resin Infusion Process. Polymers. 12(12), 2841. DOI: https://doi.org/10.3390/polym12122841

[16] Praveena, B.A., Santhosh, N., Buradi, A., et al., 2022. Experimental Investigation on Density and Volume Fraction of Void, and Mechanical Characteristics of Areca Nut Leaf Sheath Fiber-Reinforced Polymer Composites. International Journal of Polymer Science. 2022, 1–13. DOI: https://doi.org/10.1155/2022/6445022

[17] Dehury, J., Mohanty, J., 2021. Study of Physico-Mechanical Behaviour of Alkali Treated Date Palm Petiole Fiber/Epoxy Composites. In: Pal, S., Roy, D., Sinha, S.K. (Eds.). Processing and Characterization of Materials, Springer Proceedings in Materials. Springer: Singapore. pp. 305–314. DOI: https://doi.org/10.1007/978-981-16-3937-1_32

[18] United Nations, 2015. Transforming Our World: The 2030 Agenda for Sustainable Development. United Nations: New York, NY, USA. Available from: https://sdgs.un.org/2030agenda

[19] Alfonso, I., Figueroa, I.A., Rodriguez-Iglesias, V., et al., 2016. Estimation of elastic moduli of particulate-reinforced composites using finite element and modified Halpin–Tsai models. Journal of the Brazilian Society of Mechanical Sciences and Engineering. 38(4), 1317–1324. DOI: https://doi.org/10.1007/s40430-015-0429-y

[20] Akhter, M.A., Mondal, D., Debnath, A.K., et al., 2025. Evaluation of mechanical and thermal performance of jute and coconut fiber-reinforced epoxy composites with rice husk ash for wall insulation applications. Heliyon. 11(3), e42211. DOI: https://doi.org/10.1016/j.heliyon.2025.e42211

[21] Chai, T., Draxler, R.R., 2014. Root mean square error (RMSE) or mean absolute error (MAE)?—Arguments against avoiding RMSE in the literature. Geoscientific Model Development. 7(3), 1247–1250. DOI: https://doi.org/10.5194/gmd-7-1247-2014

[22] Pickering, K.L., Efendy, M.G.A., Le, T.M., 2016. A review of recent developments in natural fibre composites and their mechanical performance. Composites Part A: Applied Science and Manufacturing. 83, 98–112. DOI: https://doi.org/10.1016/j.compositesa.2015.08.038

[23] ASTM International, 2022. ASTM D638-22, Standard Test Method for Tensile Properties of Plastics. ASTM International: West Conshohocken, PA, USA. Available from: https://storethinghiem.vn/uploads/files/D%20638%20-%2022.pdf

[24] Betelie, A.A., Sinclair, A.N., Kortschot, M., et al., 2019. Mechanical properties of sisal-epoxy composites as functions of fiber-to-epoxy ratio. AIMS Materials Science. 6(6), 985–996. DOI: https://doi.org/10.3934/matersci.2019.6.985

[25] Covallane, K., Johan, D., Singh, R.K., et al., 2025. Experimental and Numerical Investigation of Jute Fibre-Reinforced Composite, a Sustainable Material for Green Energy. In: Proceedings of the 4th International Conference on Future Technologies in Manufacturing, Automation, Design, and Energy 2024 (ICOFT 2024), Karaikal, India, 12–13 November 2024; p. 17. DOI: https://doi.org/10.3390/engproc2025095017

[26] Rafiquzzaman, M., Zannat, M., Islam, M.T., et al., 2022. An Experimental and Numerical Approach of Polymer Composites Based on Jute-Bamboo Natural Fiber. Mechanics of Advanced Composite Structures. 9(1), 105–113. DOI: https://doi.org/10.22075/macs.2022.20908.1277